

## PAPER

# Understanding C–C bond formation in polar reactions. An ELF analysis of the Friedel–Crafts reaction between indoles and nitroolefins

Cite this: *RSC Advances*, 2013, 3, 7520

Luis R. Domingo,<sup>\*a</sup> Patricia Pérez<sup>b</sup> and José A. Sáez<sup>c</sup>

The Friedel–Crafts (FC) reaction of *N*-methyl indole **1** with nitroethylene **2** has been studied using DFT methods at the B3LYP/6-31+G\*\* level in order to characterize the bonding changes along the C–C bond-formation process in polar reactions. For this FC reaction a two-step mechanism has been found. The first step is associated with the C–C bond formation between the most electrophilic centre of nitroethylene and the most nucleophilic centre of *N*-methyl indole, to yield a zwitterionic intermediate **IN**. The second step corresponds to an intramolecular proton transfer process at **IN**, regenerating the aromatic system present at the indole. Despite the high electrophilic character shown by nitroethylene **2**, the electrophilic attack is not favoured, and the FC reaction is experimentally catalyzed by a bisamide. ELF bonding analysis along the first step provides a complete characterization of the electron density changes along the C–C bond formation, which begins at a distance of 1.97 Å by a C-to-C coupling of *two pseudoradical* centres located at the most electrophilic centre of nitroethylene complex **10** and the most nucleophilic centre of *N*-methyl indole **1**. Our proposed reactivity model for the C–C bond formation in polar processes is completely different to that proposed by the FMO theory, in which the HOMO electrons of the nucleophile must interact with the LUMO of the electrophile.

Received 24th December 2012,  
Accepted 28th February 2013

DOI: 10.1039/c3ra40929e

www.rsc.org/advances

## Introduction

Addition of nitroolefins to heteroaromatic compounds, through a Friedel–Crafts (FC) type reaction, is an important C–C bond-formation process in organic chemistry for the synthesis of valuable building blocks (see Scheme 1).<sup>1</sup> As nitroolefins are not sufficiently electrophilically activated to initiate an electrophilic aromatic substitution (EAS), these reactions are normally performed using Lewis acids<sup>2</sup> or organocatalysts.<sup>3</sup>

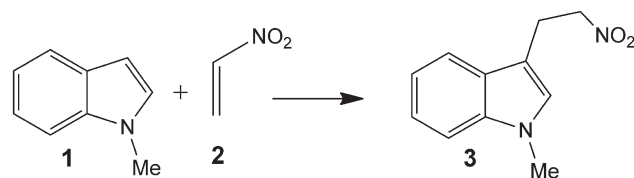
Hydrogen-bonding interactions play a crucial role in some organocatalytic enantioselective reactions.<sup>4</sup> In this sense, some FC-type alkylations of nitroolefins using L-proline and their derivatives,<sup>5</sup> chiral ureas<sup>6</sup> and cinchona alkaloids<sup>7</sup> have been reported. Furthermore, vicinal diamine derivatives have been intensively used in asymmetric synthesis due to their important role as chiral ligands in Lewis acid complexes.<sup>8</sup>

Accordingly, Jørgensen *et al.*<sup>9</sup> reported the use of chiral bis-sulfonamide catalysts, such as **6**, in enantioselective reactions

of *N*-methyl indole **1** with nitrostyrenes **4**, yielding FC adducts **5** (see Scheme 2). Formation of hydrogen bonds between the acidic hydrogen of the sulfonamide groups of **6** with the two oxygen atoms of nitrostyrenes **4** was crucial to facilitate the FC reaction.

Organic reactions involving the formation of a new C–C bond between molecules of opposite electronic nature (electrophile and nucleophile) are essential in the arsenal of organic chemists since they enable the construction of the carbon skeleton of complex organic molecules.

Within the frontier molecular orbital (FMO) theory,<sup>10</sup> bond-formation processes in polar reactions have been proposed that take place *via* an electron-donation from the HOMO of the nucleophile to the virtual LUMO of the electrophile. Analysis of the HOMO coefficients in the nucleophile and the LUMO ones in the electrophile has been used to explain regio- and



Scheme 1

<sup>a</sup>Universidad de Valencia, Departamento de Química Orgánica, Dr Moliner 50, E-46100 Burjassot, Valencia, Spain. E-mail: domingo@utopia.uv.es ; Web: www.luisrdomingo.com

<sup>b</sup>Universidad Andrés Bello, Facultad de Ciencias Exactas, Departamento de Ciencias Químicas, Laboratorio de Química Teórica, Av. República 275, 8370146 Santiago, Chile

<sup>c</sup>Instituto de Tecnología Química UPV-CSIC, Camino de Vera s/n, 46022 Valencia, Spain

chemoselectivity in polar reactions.<sup>11</sup> However, we have very recently shown that the FMO model is wrong as the energy level of the virtual LUMO is too high to be reached by HOMO electrons under commonly used experimental reaction conditions.<sup>12</sup>

We have performed an extensive study on the mechanism of Diels–Alder reactions,<sup>13</sup> finding a very good correlation between the polar character and the feasibility of the reaction, enabling the classification of polar Diels–Alder (P-DA) reactions.<sup>14</sup> Most P-DA reactions involving asymmetric electrophiles such as nitroethylene **2** take place *via* a two-stage one-step mechanism through highly asymmetric transition state structures (TSs) (see Scheme 3).<sup>14</sup>

In addition, recent theoretical studies have shown that the topological analysis of the electron localization function<sup>15</sup> (ELF) along the reaction path is a valuable tool for understanding the bonding changes.<sup>16</sup> A number of ELF bonding analyses along the intrinsic reaction coordinates (IRC) associated with polar reactions have indicated that the C–C bond formation takes place *via* a C-to-C *pseudodiradical* coupling between the most nucleophilic and electrophilic centres of these reagents, which have monosynaptic basins with some electron density (see monosynaptic basins in green in **TSno** in Fig. 1).<sup>12,17</sup> Interestingly, the electron-density changes demanded for C–C bond formations are facilitated by the global charge transfer (CT) that takes place from the nucleophile to the electrophile (see the blue arrow in **TSno** in Fig. 1).<sup>17b</sup> Because the most favorable **TSno** can be associated with a Michael-type addition of the enamine **7** to the conjugated position of nitroethylene **2**, we propose that the C-to-C *pseudodiradical* coupling pattern can be generalized to any polar reaction involving the C–C bond formation between two  $\pi$  systems.

Herein, the FC reaction between *N*-methyl indole **1** and nitroethylene **2** in the presence of the acidic tetrafluoroglycol (TFG) **9**, as a reduced model of the chiral bis-sulphonamide **6** experimentally used by Jørgensen *et al.*,<sup>9</sup> is studied (see Scheme 4). An ELF bonding analysis along the C–C bond-formation step is performed in order to achieve a complete characterization of the electronic changes in the C–C bond formation in polar reactions, and thus, generalize our reactivity model of C–C bond formation.

### Computational details

DFT calculations were carried out using the B3LYP<sup>18</sup> exchange–correlation functionals, together with the standard

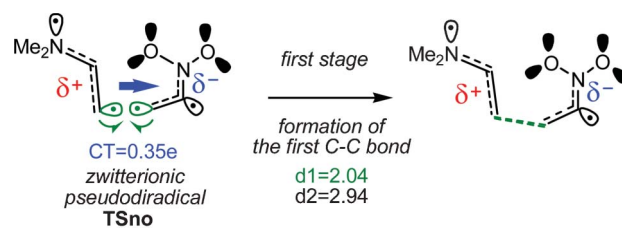
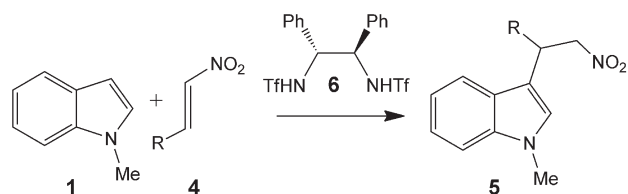


Fig. 1 C–C bond formation in the hetero-Diels–Alder reaction between nitroethylene **2** and *N,N*-dimethyl vinyl amine **7** (see Scheme 3).

6-31+G\*\* basis set.<sup>19</sup> Optimizations were carried out using the Berny analytical gradient optimization method.<sup>20</sup> Stationary points were characterized by frequency calculations in order to verify that TSs have one and only one imaginary frequency. IRC<sup>21</sup> paths were traced in order to check the energy profiles connecting each TS to the two associated minima of the proposed mechanism using the second order González–Schlegel integration method.<sup>22</sup> Solvent effects of dichloromethane (DCM) were taken into account through full optimisations using the polarisable continuum model (PCM) as developed by Tomasi's group<sup>23</sup> in the framework of self-consistent reaction field (SCRF).<sup>24</sup> The electronic structures of stationary points were analyzed by the natural bond orbital (NBO) method<sup>25</sup> and by the ELF topological analysis,  $\eta(\mathbf{r})$ .<sup>15</sup> The ELF study was performed with the TopMod program<sup>26</sup> using the corresponding monodeterminantal wavefunctions of the selected structures of the IRC. All calculations were carried out with the Gaussian 09 suite of programs.<sup>27</sup> The MPWB1K<sup>28</sup> hybrid meta functional was used to obtain reliable thermochemical values (see later).

The global electrophilicity index,<sup>29</sup>  $\omega$ , is given by the following simple expression,<sup>29</sup>  $\omega = (\mu^2/2\eta)$ , in terms of the electronic chemical potential  $\mu$ <sup>30</sup> and the chemical hardness  $\eta$ .<sup>30</sup> Both quantities may be approached in terms of the one electron energies of the frontier molecular orbital HOMO and LUMO,  $\varepsilon_H$  and  $\varepsilon_L$ , as  $\mu \approx (\varepsilon_H + \varepsilon_L)/2$  and  $\eta \approx (\varepsilon_L - \varepsilon_H)$ , respectively.<sup>30</sup> Recently, we have introduced an empirical (relative) nucleophilicity index,<sup>31</sup>  $N$ , based on the HOMO energies obtained within the Kohn–Sham scheme<sup>32</sup> and defined as  $N = E_{\text{HOMO}}(\text{Nu}) - E_{\text{HOMO}}(\text{TCE})$ . Nucleophilicity refers to tetracyanoethylene (TCE), as it presents the lowest HOMO energy in a large series of molecules already investigated in the context of polar cycloadditions. This choice allows us to conveniently handle a nucleophilicity scale of positive values.<sup>31a</sup>



Scheme 2



Scheme 3

The electrophilic,  $P_k^+$ , and nucleophilic,  $P_k^-$ , Parr functions,<sup>33</sup> were obtained through the analysis of the Mulliken atomic spin density (ASD) of the radical anion and the radical cation by single-point energy calculations over the optimized neutral geometries using the unrestricted UB3LYP formalism for radical species. With these values at hand, local electrophilicity indices,<sup>34</sup>  $\omega_k$ , and the local nucleophilicity indices,<sup>35</sup>  $N_k$ , were evaluated using the following expressions:<sup>33</sup>  $\omega_k = \omega P_k^+$  and  $N_k = NP_k^-$ .

## Results and discussions

In order to establish the nature of the C–C bond formation in FC reactions, i) an analysis of the reagents based on DFT reactivity descriptors will be performed; ii) then, a mechanistic study of the FC reaction between *N*-methyl indole **1** and nitroethylene complex **10** will be undertaken to characterise the C–C bond-formation step, and iii) finally an ELF bonding analysis along the C–C bond-formation step in this FC reaction will be carried out in order to establish the nature of the bond formation in these polar reactions.

### Analysis of the global and local reactivity indices at the ground state of the reagents

Analysis of the reactivity indices defined within the conceptual DFT<sup>36</sup> allows for the establishment of the non-polar or polar nature of a reaction.<sup>37</sup> Along a polar reaction, an amount of electron density is transferred from the nucleophile to the electrophile, a behaviour that can be easily anticipated by the analysis of the electrophilicity,<sup>29</sup>  $\omega$ , and nucleophilicity,<sup>31</sup>  $N$ , indices of the reagents. The static global properties of the reagents involved in the C–C bond-formation step of the FC reaction between *N*-methyl indole **1** and nitroethylene complex **10**, namely electronic chemical potential ( $\mu$ ), chemical hardness ( $\eta$ ), global electrophilicity ( $\omega$ ), and global nucleophilicity ( $N$ ), computed at B3LYP/6-31G\* level are shown in Table 1.

The electronic chemical potential of *N*-methyl indole **1**,  $\mu = -2.66$  eV, is higher than that of nitroethylene **2**,  $\mu = -5.33$  eV, and nitroethylene complex **10**,  $\mu = -6.04$  eV, indicating that the CT along the corresponding polar reactions will take place from the electron rich *N*-methyl indole **1** towards nitroethylene **2** and complex **10**.

The electrophilicity  $\omega$  of *N*-methyl indole **1** is 0.68 eV, being classified as a marginal electrophile on the electrophilicity scale.<sup>37a</sup> On the other hand, indole **1** has a high nucleophilicity index,  $N = 3.83$  eV, thus being classified as a strong

**Table 1** B3LYP/6-31G\* electronic chemical potential ( $\mu$ ), chemical hardness ( $\eta$ ), global electrophilicity ( $\omega$ ), and global nucleophilicity ( $N$ ), in eV, of *N*-methyl indole **1**, nitroethylene **2**, nitroethylene complex **10**, and Jørgensen's nitroethylene (2):bisamide (**6**) complex **11**

	$\mu$	$\eta$	$\omega$	$N$
<b>11</b>	-5.12	3.13	4.18	2.44
<b>10</b>	-6.04	4.60	3.96	0.78
<b>2</b>	-5.33	5.44	2.61	1.07
<b>1</b>	-2.66	5.24	0.68	3.83

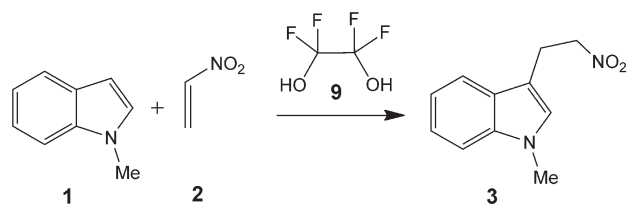
nucleophile within the nucleophilicity scale.<sup>38</sup> Consequently, *N*-methyl indole **1** may act only as a strong nucleophile.

The electrophilicity  $\omega$  of nitroethylene **2** is 2.61 eV, being classified as a strong electrophile. On the other hand, **2** has a low nucleophilicity index,  $N = 0.78$  eV, thus being classified as a marginal nucleophile. Therefore, nitroethylene **2** may act only as a strong electrophile. Formation of nitroethylene complex **10** by formation of two hydrogen bonds with TFG **9** considerably enhances the electrophilicity of nitroethylene **2** to 3.96 eV. The global indices for Jørgensen's nitroethylene (2):bisamide (**6**) complex **11** are also included in Table 1. It can be seen that the electrophilicity value of bisamide complex **11** is slightly higher than that of nitroethylene complex **10**, even though the nucleophilic character is lower than that of the same reference complex. Therefore the electrophilic character of Jørgensen's complex **11** appears to be well represented by using our model **10**.

For simple molecules, we have proposed that the  $\Delta\omega$  between reagents involved in the reaction could be considered as a measure of the polar character of the reactions.<sup>37a</sup> Formation of hydrogen-bonded complex **10** raises the  $\Delta\omega$  of EAS reaction from  $\Delta\omega = 1.93$  eV for the uncatalyzed process to  $\Delta\omega = 3.28$  eV for the catalyzed one.<sup>39</sup> This behaviour, which is similar to that observed in Lewis acid catalyzed processes, provides an explanation of the catalytic role of the amides, such as **6**, to produce a strong electrophilic activation of nitroethylene **2** by means of formation of two hydrogen bonds with the oxygen atoms of the nitro group.

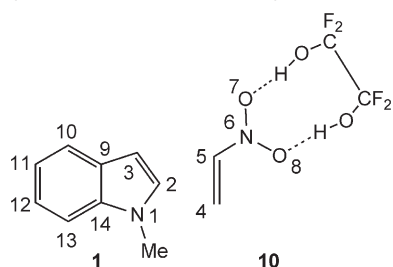
Along a polar cycloaddition involving asymmetric reagents, the most favourable reactive channel is that involving the initial two-centre interaction between the most electrophilic and nucleophilic centre of both reagents. Recently, we have proposed the electrophilic,  $P_k^+$ , and nucleophilic,  $P_k^-$ , Parr functions<sup>33</sup> derived from the excess of spin electron density reached *via* a global CT process from the nucleophile towards the electrophile. Analysis of these functions accounts for the most favourable C–C bond formation *via* a C-to-C *pseudodiradical* coupling at the most electrophilic and nucleophilic centres of the reagents. The electrophilic,  $P_k^+$ , and nucleophilic,  $P_k^-$ , Parr functions, and the corresponding local electrophilicity indices,  $\omega_k$ , and the local nucleophilicity,  $N_k$ , of nitroethylene complex **10**, and *N*-methyl indole **1** are given in Table 2.

Nucleophilic  $P_k^-$  Parr functions of *N*-methyl indole **1** show that the C3 carbon is the most nucleophilic activated centre,  $P_k^- = 0.38$ , in clear agreement with the regioselectivity experimentally observed in the EAS reactions of indole.<sup>9</sup> C10



Scheme 4

**Table 2** Electrophilic,  $P_k^+$ , and nucleophilic,  $P_k^-$ , Parr functions, and the corresponding local electrophilicity indices,  $\omega_k$ , and the local nucleophilicity,  $N_k$ , in eV, of nitroethylene complex **10**, and *N*-methyl indole **1**



		$P_k^-$	$N_k$			$P_k^+$	$\omega_k$	
<b>1</b>	N1	0.23	0.90	<b>10</b>	C4	0.42	1.68	
	C2	0.01	0.05		C5	-0.06	-0.25	
	C3	0.38	1.47		N6	0.29	1.16	
	C9	-0.11	-0.42		O7	0.23	0.90	
	C10	0.27	1.04		O8	0.17	0.66	
	C11	-0.02	-0.08					
	C12	0.10	0.39					
	C13	0.19	0.74					
	C14	-0.04	-0.16					

and C12 positions located in the benzene ring, and the indolic N1 nitrogen are also nucleophilically activated. Interestingly, the C9 carbon, which is between the C3 and C10 nucleophilically activated centres, is strongly deactivated. On the other hand, electrophilic  $P_k^-$  Parr functions of nitroethylene complex **10** indicate that the C4 carbon is the most electrophilic centre of this complex,  $P_k^+ = 0.42$ . Note that all three heteroatoms belonging to the nitro group are also electrophilically activated.

Analysis of the local reactivity indices indicates that while the C3 carbon is the most nucleophilic centre of *N*-methyl indole **1**,  $N_{C3} = 1.47$  eV, the C4 carbon is the most electrophilic centre of nitroethylene complex **10**  $\omega_{C4} = 1.68$  eV. Accordingly, along the first step of the FC reaction between nucleophilic *N*-methyl indole **1** and electrophilic nitroethylene complex **10**, the most favourable two-centre interaction will take place between the C3 carbon of indole **1** and the C4 carbon of nitroethylene complex **10**, in clear agreement with the regioselectivity experimentally observed.

### Mechanistic study of the FC reaction between *N*-methyl indole **1** and nitroethylene complex **10**

The mechanistic study of the FC reaction between *N*-methyl indole **1** and nitroethylene complex **10** was performed using the B3LYP functional together with the 6-31+G\*\* basis set. Preliminary studies using the standard 6-31G\* basis set were unsuccessful since the corresponding zwitterionic intermediate was unstable, even after including solvent effects. Similar results were obtained using the M06-2X functional.<sup>40</sup>

The FC reaction between *N*-methyl indole **1** and nitroethylene complex **10**, which corresponds to an EAS reaction between electrophilic activated nitroethylene complex **10** and the aromatic indole **1**, takes place through a two-step mechanism (see Scheme 5). The first step corresponds to the

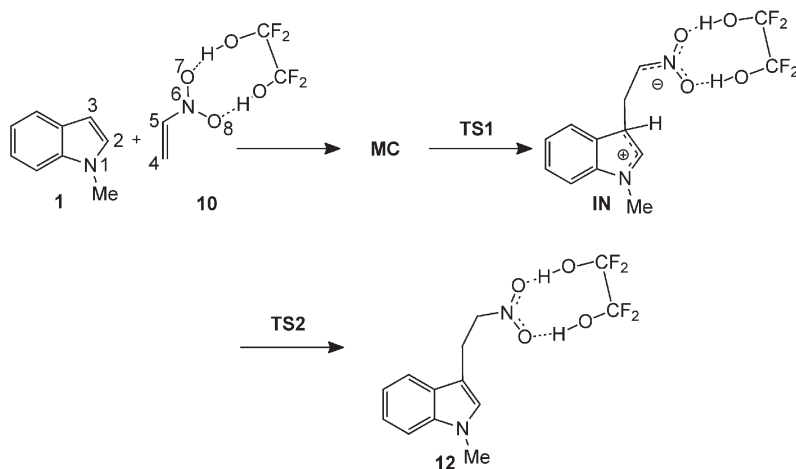
C3–C4 bond formation through the electrophilic approach of the C4 carbon of the activated nitroethylene complex **10** to the C3 position of *N*-methyl indole **1**, yielding the zwitterionic intermediate **IN**, *via* **TS1**. In the second step, a proton abstraction process at the C3 position of the corresponding indolium moiety regenerates the aromatic ring present in indole **1**. Although this step usually is a bimolecular process promoted by a basic species, in this Michael-type addition, the anionic fragment present in the nitroethylene framework may facilitate the intramolecular process, yielding the final Michael adduct **12**, *via* **TS2**. The total and relative energies, in gas phase and in DCM, of the stationary points involved in the FC reaction between *N*-methyl indole **1** and nitroethylene complex **10** are given in Table 3. Since some species involved in the FC reactions have a strong zwitterionic character, energy discussion will be done using DCM energies.

The IRC from **TS1** to the reagents stops in a molecular complex, **MC**, in which the two planar  $\pi$  systems of both reagents are in parallel rearrangement with a distance of 3.57 Å. Formation of **MC** in gas phase is exothermic by  $-2.5$  kcal mol<sup>-1</sup>, however in DCM this complex is stabilized by  $-10.7$  kcal mol<sup>-1</sup>. **MC** will be used as the reference energy, since **TS1** and **IN** in DCM are located below the separated reagents. The activation energy associated to **TS1** is 7.0 kcal mol<sup>-1</sup>, and formation of zwitterionic intermediate **IN** in DCM is exothermic by  $-5.6$  kcal mol<sup>-1</sup>. Therefore, the first step of this hydrogen-bond catalyzed FC reaction is kinetically favourable.

The intramolecular proton abstraction in zwitterionic intermediate **IN** *via* **TS2** has a high activation energy, 30.0 kcal mol<sup>-1</sup>, mainly due to the strain associated with the four membered **TS**.<sup>41</sup> Any basic species present in the reaction could reduce this unfavourable barrier. Nevertheless, the overall reaction is very exothermic by  $-32.9$  kcal mol<sup>-1</sup>, the formation of FC adduct **12** being irreversible.

The geometries of the **TSs** involved in this FC reaction are given in Fig. 2. At **TS1**, the length of the C3–C4 forming bond is 1.809 Å. This short distance indicates that this **TS** is very advanced (see below). Note that at intermediate **IN**, the length of the C3–C4 bond is 1.664 Å. At **TS1**, the O7–H and O8–H distances associated with the hydrogen-bonds are 1.707 and 1.679 Å, respectively. These very short distances point to strong hydrogen-bond interactions. Note that at nitroethylene complex **10**, these distances are 1.998 and 1.991 Å, respectively. At **TS2**, the lengths of the C3–H breaking and C4–H forming bonds are 1.342 and 1.574 Å, respectively. At this **TS**, the O7–H and O8–H hydrogen-bonds are slightly longer than those at **TS1**, due to the loss of the zwitterionic character of **TS2** owing to the proton transfer process. Note that the dipolar moments of **TS1** and **TS2** are 18.0 and 14.3 Debye, respectively.

Finally, the analysis of the natural atomic charges at **TS1** indicates that an electron density of 0.60e is being globally transferred from the nucleophilic *N*-methyl indole **1** to the electrophilically activated nitroethylene complex **10**. This high value, which reaches 0.73e at intermediate **IN**, accounts for the very strong polar character of this FC reaction.



Scheme 5

### ELF bonding analysis along the C–C bond-formation step in the FC reaction between *N*-methyl indole **1** and nitroethylene complex **10**

A topological analysis of the ELF along the C–C bond-formation step in the FC reaction between *N*-methyl indole **1** and nitroethylene complex **10** was performed in order to understand the bond formation in this polar reaction. The most relevant ELF valence basins and their corresponding *N* populations of the points belonging to the different phases are displayed in Table 4. A schematic representation of the bonding changes along the different phases involved in this cycloaddition reaction is given in Fig. 3. Attractor positions and atomic numbering for the most relevant points are shown in Fig. 4.

Analysis of ELF basin populations along the IRC of the FC reaction between indole **1** and nitroethylene complex **10** allows for the characterization of ten phases (see Table 4). At *phase I*,  $3.00 \geq d(\text{C3}–\text{C4}) > 2.44 \text{ \AA}$ , the ELF picture of the N1–C2–C3 framework of *N*-methyl indole **1** reveals two monosynaptic basins  $V(\text{N1})$  and  $V'(\text{N1})$ , integrating 0.96e and 0.66e, respectively, which are associated with the lone pairs present at the N1 nitrogen, and two disynaptic basins  $V(\text{N1},\text{C2})$  and  $V(\text{C2},\text{C3})$ , integrating to 2.07e and 3.40e, respectively. Nitroethylene complex **10** shows two disynaptic basins

$V(\text{C4},\text{C5})$  and  $V'(\text{C4},\text{C5})$  associated with the C4–C5 double bond, whose electronic populations integrate 1.74e and 1.73e, one disynaptic basin  $V(\text{C5},\text{N6})$  associated with the C5–N6 bond, whose electronic population integrates 2.80e, two disynaptic basins  $V(\text{N6},\text{O7})$  and  $V(\text{N6},\text{O8})$  associated with the two N6–O bonds, whose electronic populations integrate 1.71e and 1.74e, and two pairs of monosynaptic basins,  $V(\text{O7})$ ,  $V'(\text{O7})$ ,  $V(\text{O8})$  and  $V'(\text{O8})$ , each pair integrating 5.76 and 5.77e, respectively. At this point of the IRC the CT is 0.06e. The above-mentioned results indicate a large polarization of nitroethylene complex **10** towards the two O7 and O8 oxygen atoms. Along the IRC, while the populations of the disynaptic basins  $V(\text{N6},\text{O7})$  and  $V(\text{N6},\text{O8})$  decrease to 1.46 and 1.49e, the population of the two pairs of oxygen monosynaptic basins increase to 6.03 and 5.97e.

In *phase II*,  $2.44 \geq d(\text{C3}–\text{C4}) > 2.41 \text{ \AA}$  only changes in electron density are observed. At the end of this phase the CT rises to 0.19. At *phase III*,  $2.41 \geq d(\text{C3}–\text{C4}) > 2.17 \text{ \AA}$ , the two disynaptic basins  $V(\text{C4},\text{C5})$  and  $V'(\text{C4},\text{C5})$  present in the nitroethylene complex merge into one new disynaptic basin  $V(\text{C4},\text{C5})$ , integrating 3.41e.

The first relevant change in the IRC is found in *phase IV*,  $2.17 \geq d(\text{C3}–\text{C4}) > 2.09 \text{ \AA}$ . In this short phase, a monosynaptic

**Table 3** B3LYP/6-31+G\*\* total (*E*, in au) and relative energies ( $\Delta E$ , in kcal mol<sup>−1</sup>), in gas phase and in DCM, of the stationary points involved in the FC reaction between *N*-methyl indole **1** and nitroethylene complex **10**

	gas phase		DCM	
	<i>E</i>	$\Delta E$	<i>E</i>	$\Delta E$
<b>1</b>	−403.157450		−403.162626	
<b>10</b>	−910.397893		−910.395713	
<b>MC</b>	−1313.559296	−2.5	−1313.575348	−10.7
<b>TS1</b>	−1313.532974	14.0	−1313.564300	−3.7
<b>IN</b>	−1313.532780	14.2	−1313.582330	−15.1
<b>TS2</b>	−1313.509927	28.5	−1313.534332	15.1
<b>12</b>	−1313.596583	−25.9	−1313.610769	−32.9

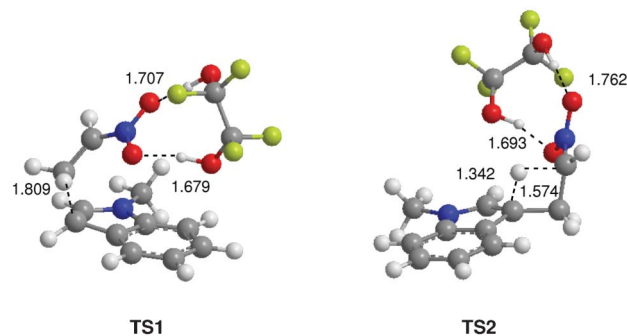


**Fig. 2** B3LYP/6-31+G\*\* geometries of the transition states involved in the FC reaction between *N*-methyl indole **1** and nitroethylene complex **10**.

**Table 4** Valence basin populations  $N$  calculated from the ELF analysis of some selected points associated with the formation of the C3–C4  $\sigma$  bond-formation step associated with the FC reaction between indole **1** and the nitroethylene complex **10**. The NBO bond orders<sup>42</sup> (BO) and the CT along the IRC is also included

	I	II	III	IV	V	VI	VII	VIII	IX	X
$d(\text{C3-C4})$	3.00	2.44	2.41	2.17	2.09	2.06	2.00	1.97	1.95	1.66
BO (NBO)	0.03	0.14	0.15	0.29	0.36	0.39	0.44	0.47	0.51	0.82
CT (NBO)	0.06	0.19	0.20	0.33	0.38	0.41	0.45	0.47	0.49	0.73
V(N1)	0.96	0.87	0.84	0.74	0.67	0.64				
V'(N1)	0.66	0.63	0.64	0.60						
V(N1,C2)	2.07	2.19	2.19	2.30	2.93	2.96	3.60	3.57	3.56	3.54
V(C2,C3)	3.40	3.24	3.23	2.93	2.81	2.77	2.71	2.67	2.63	2.26
V(C4,C5)	1.74	1.78	3.41	3.44	3.43	3.32	3.01	2.96	2.47	2.09
V'(C4,C5)	1.73	1.66								
V(C5,N6)	2.80	2.94	2.92	3.02	3.07	3.06	3.07	3.10	3.13	3.33
V(N6,O7)	1.71	1.67	1.65	1.62	1.61	1.65	1.56	1.55	1.54	1.46
V(N6,O8)	1.74	1.65	1.67	1.62	1.60	1.58	1.60	1.61	1.60	1.49
V(O7)	2.95	3.02	3.00	3.01	3.11	3.11	3.14	3.09	3.09	3.17
V'(O7)	2.81	2.78	2.79	2.81	2.85	2.82	2.89	2.85	2.85	2.86
V(O8)	2.94	2.94	2.94	3.02	2.99	3.01	3.04	3.08	3.06	3.14
V'(O8)	2.83	2.86	2.85	2.85	2.87	2.87	2.82	2.80	2.85	2.83
V(C5)							0.28	0.28	0.30	0.46
V'(C5)									0.43	0.49
V(C3)				0.31	0.41	0.45	0.57			
V(C4)						0.14	0.14			
V(C3,C4)								0.82	0.89	1.52

basin V(C3), integrating 0.31e, emerges at the most nucleophilic centre of *N*-methyl indole **1**. At this point of the IRC the CT is 0.33e. In *phase V*,  $2.09 \geq d(\text{C3-C4}) > 2.06 \text{ \AA}$ , while the monosynaptic basin V'(N1) of *N*-methyl indole **1** disappears, the disynaptic basin V(N1,C2) increases its electron density to 2.93e and the monosynaptic basin V(C3) slightly increases its population to 0.41e. The second relevant change in the IRC occurs in *phase VI*,  $2.06 \geq d(\text{C3-C4}) > 2.00 \text{ \AA}$ . In this short phase, a new monosynaptic basin V(C4), integrating 0.14e, is created at the most electrophilic centre, while the mono-

synaptic basin V(C3) reaches 0.45e. In *phase VII*,  $2.00 \geq d(\text{C3-C4}) > 1.97 \text{ \AA}$ , while the monosynaptic basin V(N1) disappears, the electron-density of the disynaptic basin V(N1,C2) increases to 3.60e. Taking into account the population of the monosynaptic basin V(N1) in *phase VI*, it appears that this monosynaptic basin has merged with the disynaptic basin V(N1,C2). At this point of the IRC, a large amount the electron density has been transferred from *N*-methyl indole **1** to nitroethylene complex **10**, the CT being 0.45e.

At the very short *phase VIII*,  $1.97 \geq d(\text{C3-C4}) > 1.95 \text{ \AA}$ , the most relevant change in bonding occurs. The two monosynaptic basins V(C3) and V(C4) merge into the new disynaptic basin V(C3,C4), which integrates 0.82e, indicating that the formation of the new C3–C4  $\sigma$  bond has started. From this phase to the formation of intermediate **IN1**, the electron-density of the disynaptic basin V(C3,C4) increases to reach 1.52e in the intermediate. At this point of IRC the CT is 0.47e.

In *phase IX*,  $1.95 \geq d(\text{C3-C4}) > 1.66 \text{ \AA}$ , a new monosynaptic basin V'(C5), integrating 0.43e, appears at the C5 carbon. Considering that the disynaptic basin V(C4–C5) has been depopulated by 0.49e, it can be assumed that this new monosynaptic basin V'(C5) comes from the transformation of the C4–C5 double bond present in nitroethylene **1** into the single bond in intermediate **IN**. Finally, in the last *phase X*,  $d(\text{C3-C4}) = 1.66 \text{ \AA}$ , the disynaptic basin V(C3,C4) reaches 1.52e with the formation of **IN**. With the formation of the zwitterionic intermediate **IN**, the CT reaches the highest value, 0.73e.

Some interesting conclusions can be drawn from this ELF analysis: i) formation of the C3–C4  $\sigma$  bond takes place through the merge of two monosynaptic basins, V(C3) and V(C4), created in earlier phases, *IV* and *VI*, respectively. These monosynaptic basins are located at the most nucleophilic centre, the C3 carbon of *N*-methyl indole **1**, and the most electrophilic centre, the C4 carbon of nitroethylene **2**, which are clearly established by the nucleophilic  $P_k^-$  and electrophilic  $P_k^+$  Parr functions; ii) the C3–C4 bond formation begins at the C3–C4 distance of  $1.97 \text{ \AA}$ , with an initial electron density of 0.82e. At the end of the IRC, when intermediate **IN** has been

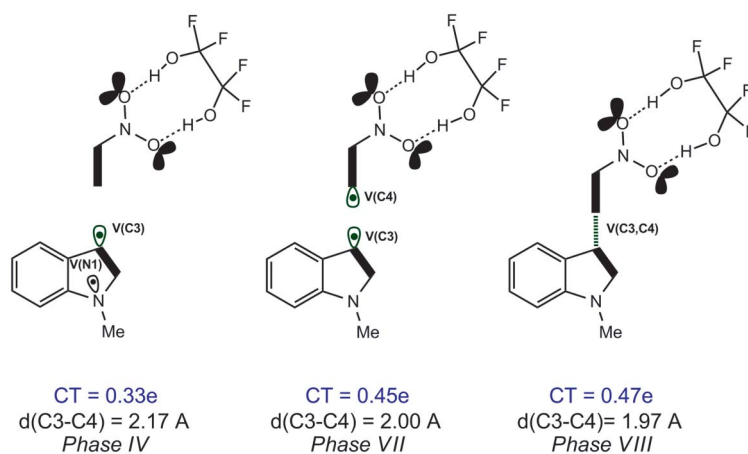


**Fig. 3** A schematic representation of most relevant disynaptic and monosynaptic basins of selected points belonging to *phases IV*, *VII* and *VIII*, of the IRC of the C–C bond-formation step in the FC reaction between *N*-methyl indole **1** and nitroethylene complex **10**, represented by full lines and by ellipses with a dot, respectively. Dotted lines indicate a low basin population, while filled ellipses indicate a high basin population.

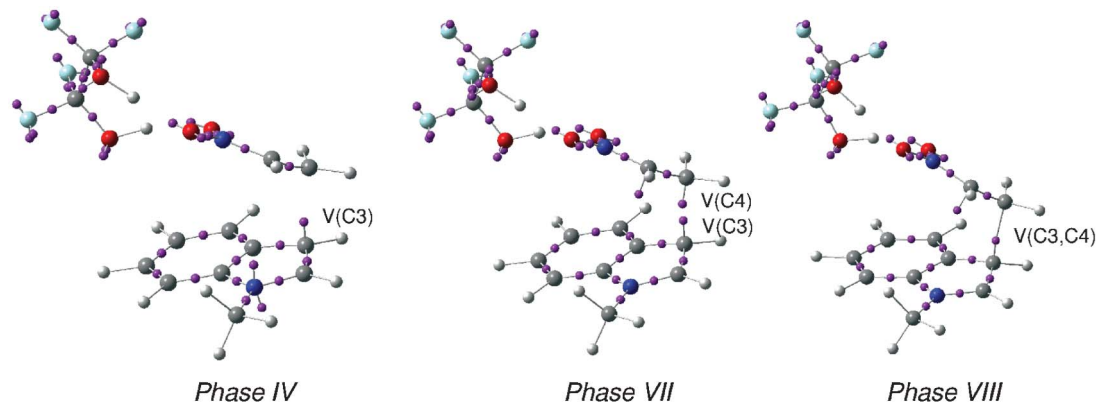


**Fig. 4** The most relevant ELF attractors at selected points of the IRC of the C–C bond-formation step in the FC reaction between *N*-methyl indole **1** and nitroethylene complex **10**.

completely formed this electron density reaches 1.52e; iii) this distance is very close to those found along the formation of the first C–C bond in P-DA reactions, in the narrow region of 2.07–1.95 Å;<sup>12,17b</sup> iv) interestingly, the TS associated with the C–C bond-formation step, **TS1**, is located at the beginning of *phase X*,  $d(\text{C4}–\text{C5}) = 1.81$  Å; consequently, at the very advanced **TS1**, the C4–C5 bond formation has already started; and iv) along the approach of nucleophilic *N*-methyl indole **1** towards electrophilic nitroethylene complex **10**, a large amount of the charge is transferred from **1** to **10**. The CT begins in *phase I*, 0.06e, and reaches 0.45e at the end of *phase VI*, before the C3–C4 bond formation. This large CT is distributed in the C=C nitroethylene framework, 0.33e, and in the NO<sub>2</sub> group, 0.21e; vi) finally, ELF bonding analysis along the C–C bond-formation step of this FC reaction indicates, as in other polar C–C bond-formation processes,<sup>12,17</sup> that it takes place *via* a C-to-C coupling between two *pseudoradical* centres characterized by the presence of two monosynaptic V(Cx) basins at the most nucleophilic and electrophilic centres of the molecules. As anticipated, these relevant points are well characterized by analysis of the electrophilic and nucleophilic Parr functions at the ground state of the molecules.

Our proposed reactivity model for the C–C bond formation in polar processes is completely different to that suggested by the FMO theory,<sup>10</sup> in which the HOMO electrons of the nucleophile must interact with the LUMO of the electrophile. Note that the HOMO<sub>nucleophile</sub>–LUMO<sub>electrophile</sub> energy gaps, usually above 50 kcal mol<sup>−1</sup>, are too large to be overcome under experimental thermic conditions.<sup>12</sup> In our proposed reactivity model, when two reagents come close to *ca.* 3.0 Å, a CT process controlled by the difference of electronic chemical potentials  $\Delta\mu$  of the reagents begins. This global CT process, which characterises polar reactions, favours the electron-reorganisation in the reagents demanded for the formation of the new C–C bond *via* a C-to-C *pseudodiradical* coupling process.

## Conclusions

The FC reaction of nitroethylene **2** with *N*-methyl indole **1** has been studied using DFT methods at the B3LYP/6-31+G\*\* in

order to characterize the bonding changes in the C–C bond-formation process in polar processes. For this FC reaction a two-step mechanism has been found. The first step is associated with the C–C bond formation between the most electrophilic centre of nitroethylene and the most nucleophilic centre of *N*-methyl indole to yield a zwitterionic intermediate. Despite the strong electrophilic character shown by nitroethylene **2**, the electrophilic attack is not favored, and the reaction must be experimentally catalyzed through the formation of a hydrogen-bonded complex of nitroethylene with a bisamide. This catalyst has been theoretically modelled using TFG. The second step corresponds to a proton abstraction in the indole framework to regenerate its aromatic system. Although this step can be carried out by any basic species present in the reaction medium, we have studied an intramolecular process yielding the final Michael adduct in an elementary step.

ELF bonding analysis along the IRC associated with the first step of this FC reaction provides a complete characterisation of the electron density changes along the C–C bond formation in this polar process. The C–C bond formation begins at a distance of 1.97 Å by the C-to-C coupling of *two pseudoradical* centres located at the most electrophilic centre of nitroethylene complex **10** and the most nucleophilic centre of *N*-methyl indole **1**. Formation of these relevant centres, which are well predicted by the recently proposed electrophilic and nucleophilic Parr functions, appears to be favored by the global CT taking place along the approach of nucleophilic *N*-methyl indole **1** towards electrophilic nitroethylene complex **10**.

This reactivity model, which is similar to that found in the C–C bond formation in P-DA reactions, is completely different to that proposed by the FMO theory, in which the HOMO electrons of the nucleophile must interact with the LUMO of the electrophile. In our proposed reactivity model, when two reagents come closer to *ca.* 3.0 Å, a CT process controlled by the difference of electronic chemical potentials  $\Delta\mu$  of the reagents begins. This global CT process, which characterizes polar reactions, favours the electron-reorganization demanded

for the formation of the new C–C bond via a C-to-C pseudodiradical coupling process.

## Acknowledgements

This work has been supported by Fondecyt grant No. 1100278. Professor L. R. Domingo thanks Fondecyt by support through the Cooperación Internacional.

## References

- (a) O. M. Berner, L. Tedeschi and D. Enders, *Eur. J. Org. Chem.*, 2002, 1877–1894; (b) M. Bandini, A. Melloni and A. Umani-Ronchi, *Angew. Chem., Int. Ed. Engl.*, 2004, **43**, 550–556.
- (a) K. Lee and D. Y. Oh, *Tetrahedron Lett.*, 1988, **29**, 2977–2978; (b) T. Ohe and S. Uemura, *Tetrahedron Lett.*, 2002, **43**, 1269–1271; (c) K. Manabe, N. Aoyama and S. Kobayashi, *Adv. Synth. Catal.*, 2001, **343**, 174–176; (d) J. S. Yadav, S. Abraham, B. V. S. Reddy and G. Sabitha, *Synthesis*, 2001, 2165–2169; (e) M. Bandini, P. Melchiorre, A. Melloni and A. Umani-ronchi, *Synthesis*, 2002, 1110–1114; (f) H. Firouzabadi, N. Iranpoor and F. Nowrouzi, *Chem. Commun.*, 2005, 789–791.
- (a) M. Bandini, M. Fagioli and A. Umani-Ronchi, *Adv. Synth. Catal.*, 2004, **346**, 545–548; (b) G. Dessole, R. P. Herrera and A. Ricci, *Synlett*, 2004, 2374.
- (a) P. M. Pihko, *Angew. Chem., Int. Ed. Engl.*, 2004, **43**, 2062–2064; (b) P. R. Schreiner, *Chem. Soc. Rev.*, 2003, **32**, 289–296; (c) P. I. Dalko and L. Moisan, *Angew. Chem., Int. Ed. Engl.*, 2004, **43**, 5138–5175.
- (a) A. J. A. Cobb, D. A. Longbottom, D. M. Shaw and S. V. Ley, *Chem. Commun.*, 2004, 1808–1809; (b) W. Wang, J. Wang and H. Li, *Angew. Chem., Int. Ed.*, 2005, **44**, 1369.
- (a) T. Okino, Y. Hoashi and Y. Takemoto, *J. Am. Chem. Soc.*, 2003, **125**, 12672–12673; (b) Y. Hoashi, T. Yabuta and Y. Takemoto, *Tetrahedron Lett.*, 2004, **45**, 9185–9188.
- (a) H. M. Li, Y. Wang, L. Tang and L. Deng, *J. Am. Chem. Soc.*, 2004, **126**, 9906–9907; (b) H. M. Li, Y. Wang, L. Tang, F. H. Wu, X. F. Liu, C. Y. Guo, B. M. Foxman and L. Deng, *Angew. Chem., Int. Ed. Engl.*, 2005, **44**, 105–108.
- D. Lucet, T. Le Gall and C. Mioskowski, *Angew. Chem., Int. Ed. Engl.*, 1998, **37**, 2581–2627.
- W. Zhuang, R. G. Hazell and K. A. Jørgensen, *Org. Biomol. Chem.*, 2005, **3**, 2566–2571.
- K. Fukui, *Molecular Orbitals in Chemistry, Physics, and Biology*, ed. P.-O. Lowdin and B. Pullman, Academic, New York, 1964.
- I. Fleming, *Frontier Orbitals and Organic Chemical Reactions*, John Wiley and Sons, Chichester, 2009.
- (a) L. R. Domingo, M. J. Aurell, P. Pérez and J. A. Sáez, *RSC Adv.*, 2012, **2**, 1334–1342; (b) L. R. Domingo, P. Pérez and J. A. Sáez, *Tetrahedron*, 2013, **69**, 107–114.
- (a) L. R. Domingo, M. Arnó and J. Andrés, *J. Org. Chem.*, 1999, **64**, 5867–5875; (b) L. R. Domingo, M. J. Aurell, P. Pérez and R. Contreras, *J. Org. Chem.*, 2003, **68**, 3884–3890.
- L. R. Domingo and J. A. Sáez, *Org. Biomol. Chem.*, 2009, **7**, 3576–3583.
- (a) A. Savin, A. D. Becke, J. Flad, R. Nesper, H. Preuss and H. G. von Schnering, *Angew. Chem., Int. Ed. Engl.*, 1991, **30**, 409–412; (b) A. Savin, B. Silvi and F. Colonna, *Can. J. Chem.*, 1996, **74**, 1088–1096; (c) A. Savin, R. Nesper, S. Wengert and T. F. Fassler, *Angew. Chem., Int. Ed. Engl.*, 1997, **36**, 1809–1832; (d) B. Silvi, *J. Mol. Struct.*, 2002, **614**, 3–10.
- (a) S. Berski, J. Andres, B. Silvi and L. R. Domingo, *J. Phys. Chem. A*, 2003, **107**, 6014–6024; (b) S. Berski, J. Andres, B. Silvi and L. R. Domingo, *J. Phys. Chem. A*, 2006, **110**, 13939–13947; (c) V. Polo, J. Andrés, R. Castillo, S. Berski and B. Silvi, *Chem.–Eur. J.*, 2004, **10**, 5165–5172; (d) V. Polo, J. Andres, S. Berski, L. R. Domingo and B. Silvi, *J. Phys. Chem. A*, 2008, **112**, 7128–7136.
- (a) L. R. Domingo, P. Pérez and J. A. Sáez, *Org. Biomol. Chem.*, 2012, **10**, 3841–3851; (b) L. R. Domingo, P. Pérez, M. J. Aurell and J. A. Sáez, *Curr. Org. Chem.*, 2012, **16**, 2343–2351.
- (a) C. Lee, W. Yang and R. G. Parr, *Phys. Rev. B*, 1988, **37**, 785–789; (b) A. D. Becke, *J. Chem. Phys.*, 1993, **98**, 5648–5652.
- W. J. Hehre, L. Radom, P. v. R. Schleyer and J. A. Pople, *Ab initio Molecular Orbital Theory*, Wiley, New York, 1986.
- (a) H. B. Schlegel, *J. Comput. Chem.*, 1982, **2**, 214–218; (b) H. B. Schlegel, in *Modern Electronic Structure Theory*, ed. D. R. Yarkony, World Scientific Publishing, Singapore, 1994.
- K. Fukui, *J. Phys. Chem.*, 1970, **74**, 4161–4163.
- (a) C. González and H. B. Schlegel, *J. Phys. Chem.*, 1990, **94**, 5523–5527; (b) C. González and H. B. Schlegel, *J. Chem. Phys.*, 1991, **95**, 5853–5867.
- (a) J. Tomasi and M. Persico, *Chem. Rev.*, 1994, **94**, 2027–2033; (b) B.Y. Simkin and I. Sheikhet, *Quantum Chemical and Statistical Theory of Solutions-A Computational Approach*, Ellis Horwood, London, 1995.
- (a) E. Cancès, B. Mennucci and J. Tomasi, *J. Chem. Phys.*, 1997, **107**, 3032–3041; (b) M. Cossi, V. Barone, R. Cammi and J. Tomasi, *Chem. Phys. Lett.*, 1996, **255**, 327–335; (c) V. Barone, M. Cossi and J. Tomasi, *J. Comput. Chem.*, 1998, **19**, 404–417.
- (a) A. E. Reed, R. B. Weinstock and F. Weinhold, *J. Chem. Phys.*, 1985, **83**, 735–746; (b) A. E. Reed, L. A. Curtiss and F. Weinhold, *Chem. Rev.*, 1988, **88**, 899–926.
- S. Noury, X. Krokidis, F. Fuster and B. Silvi, *Comput. Chem.*, 1999, **23**, 597–604.
- M. J. Frisch, *et al.*, *Gaussian 09, Revision A.01*, Gaussian, Inc., Wallingford CT, 2009.
- Y. Zhao and D. G. Truhlar, *J. Phys. Chem. A*, 2004, **108**, 6908–6918.
- R. G. Parr, L. von Szentpaly and S. Liu, *J. Am. Chem. Soc.*, 1999, **121**, 1922–1924.
- (a) R. G. Parr and R. G. Pearson, *J. Am. Chem. Soc.*, 1983, **105**, 7512–7516; (b) R. G. Parr and W. Yang, *Density Functional Theory of Atoms and Molecules*, Oxford University Press, New York, 1989.
- (a) L. R. Domingo, E. Chamorro and P. Pérez, *J. Org. Chem.*, 2008, **73**, 4615–4624; (b) L. R. Domingo and P. Pérez, *Org. Biomol. Chem.*, 2011, **9**, 7168–7175.
- W. Kohn and L. J. Sham, *Phys. Rev.*, 1965, **140**, 1133–1138.
- L. R. Domingo, P. Pérez and J. A. Sáez, *RSC Adv.*, 2013, **3**, 1486–1494.
- L. R. Domingo, M. J. Aurell, P. Pérez and R. Contreras, *J. Phys. Chem. A*, 2002, **106**, 6871–6875.



- 35 P. Pérez, L. R. Domingo, M. Duque-Noreña and E. Chamorro, *THEOCHEM*, 2009, **895**, 86–91.
- 36 (a) P. Geerlings, F. De Proft and W. Langenaeker, *Chem. Rev.*, 2003, **103**, 1793–1873; (b) D. H. Ess, G. O. Jones and K. N. Houk, *Adv. Synth. Catal.*, 2006, **348**, 2337–2361.
- 37 (a) L. R. Domingo, M. J. Aurell, P. Pérez and R. Contreras, *Tetrahedron*, 2002, **58**, 4417–4423; (b) P. Pérez, L. R. Domingo, M. J. Aurell and R. Contreras, *Tetrahedron*, 2003, **59**, 3117–3125.
- 38 P. Jaramillo, L. R. Domingo, E. Chamorro and P. Pérez, *THEOCHEM*, 2008, **865**, 68–72.
- 39 L. R. Domingo and J. Andrés, *J. Org. Chem.*, 2003, **68**, 8662–8668.
- 40 Y. Zhao and D. G. Truhlar, *Theor. Chem. Acc.*, 2008, **120**, 215.
- 41 L. R. Domingo, M. T. Picher and R. J. Zaragoza, *J. Org. Chem.*, 1998, **63**, 9183–9189.
- 42 K. B. Wiberg, *Tetrahedron*, 1968, **24**, 1083–1096.